

Statistics of Coulomb blockade peak spacings for a partially open dot

A. Kaminski and L.I. Glazman

Theoretical Physics Institute, University of Minnesota, Minneapolis, MN 55455

We show that randomness of the electron wave functions in a quantum dot contributes to the fluctuations of the positions of the conductance peaks. This contribution grows with the conductance of the junctions connecting the dot to the leads. It becomes comparable with the fluctuations coming from the randomness of the single particle spectrum in the dot while the Coulomb blockade peaks are still well-defined. In addition, the fluctuations of the peak spacings are correlated with the fluctuations of the conductance peak heights.

PACS numbers: 73.23.-b, 73.23.Hk, 73.40.Gk

I. INTRODUCTION

Quantum dot in the Coulomb blockade regime is conventionally described by the constant interaction model.¹ In this model, the Hamiltonian of the system is represented by a sum of two terms. The first one is the electrostatic charging energy, that does not fluctuate and depends on the total number of electrons only; the second term is the Hamiltonian of free quasiparticles (all interactions except the charging energy are ignored). For a disordered or chaotic quantum dot, free quasiparticles inside the dot are described by the random matrix theory (RMT).² The spectrum of quasiparticles is random, with the level spacings obeying the Wigner-Dyson statistics. The one-particle wave functions are also random, and their statistical properties within the RMT theory are defined by the Porter-Thomas distribution.

The predictions of this model may be checked in transport experiments with a dot weakly coupled by point contacts to the electron reservoirs (leads). The number of electrons on the dot in this setup is nearly quantized, and can be controlled by an additional electrode, gate, which is capacitively coupled to the dot. The dependence of the tunnel conductance through the system, G , on the gate voltage V_g exhibits sharp peaks. A Coulomb blockade peak corresponds to a point where the ground state of the dot is degenerate: the states with n and $n+1$ electrons have the same energy. The $(n+1)$ st electron can therefore freely tunnel to and from the dot, so $G(V_g)$ has a peak at this point.

For an almost closed dot, the height of the peak is related to the values of the wave functions at the points of contacts.³ The randomness of the wave functions translates into the randomness of the peak heights. The existing experimental results⁴ for the peak conductance distribution function are in a satisfactory agreement with the theory predictions.³

In the framework of the constant interaction model, the spacings between the conductance peaks contain two contributions. The first one is due to the charging energy, and does not fluctuate. The second term in the limit of weak dot-lead tunneling is proportional to the spacing between the discrete energy levels of the RMT Hamilto-

nian. This term does fluctuate, and obeys the Wigner-Dyson statistics. However, the experimentally measured distribution of peak spacings is similar to Gaussian,⁵⁻⁷ in apparent disagreement with the predictions of the constant interaction model. One of the possible explanations of this phenomenon is that the electron-electron interaction, which is not accounted for by RMT, substantially affects the dot's spectrum.⁸ Another explanation refers to the change in the dot shape with the variation of the gate voltage V_g , so the two adjacent peaks in the $G(V_g)$ dependence correspond to two different realizations of the random Hamiltonian.⁹

The above-mentioned works concentrated on the almost closed dots, when the tunnel junctions are used only as probes, without affecting the states in the dot. In the recent experiment¹⁰ the statistics of peak spacings was studied for a partially open quantum dot. In such a system, charge quantization is lifted gradually, while the conductance of the dot-lead contacts increases. Simultaneously, a crossover occurs between the sharp Coulomb blockade peaks and conductance fluctuations of relatively small amplitude in an almost open dot. The main part of the peak spacing comes from the charging energy. Therefore lifting of the charge quantization may yield an additional significant contribution to the peak spacing fluctuations. This many-body problem was not addressed theoretically by now.

In this paper, a theory of the fluctuations of the peak positions in the case of a partially open dot is developed. In Sections II and III we consider the regime in which the conductances of the dot-lead point contacts are not negligible, but still considerably smaller than the quantum unit $G_0 \equiv e^2/\pi\hbar$. Under these conditions, the conductance peaks remain well-defined. However, their positions are already affected by the finite dot-lead coupling. The randomness of the electron wave functions controlling the coupling, contributes to the fluctuations of the peak spacing. We calculate the variance of this contribution, and show that it increases with the junction conductance. We study the fluctuations of spacings between the adjacent, as well as between distant peaks. This theory allows us to form a consistent understanding of the experimental results^{7,10} for the moderate values of junction conductances.

In Section IV we consider qualitatively the case of an (almost) open dot, when the conductance of one of the contacts is close to G_0 . In this case, the $G(V_g)$ function does not exhibit sharp peaks. Nevertheless, the question regarding the fluctuations of the distance between the conductance maxima is still valid. We study the origin of these fluctuations and estimate their variance. Furthermore, we extend the consideration to the region of intermediate values of the junction conductances. In this region, the peak-to-valley ratio of the $G(V_g)$ dependence is large, but peaks are not sharp (their width exceeds the level spacing in the dot). Thus the developed theory yields understanding of the evolution of the peak spacing fluctuations with the strength of the dot-lead coupling, ranging from weak tunneling to weak reflection in the contacts between the dot and the leads.

In this paper, we base our statistical description of the electron states in the dot on the random matrix theory. Despite the apparent failure of RMT in explaining the peak spacing fluctuations in a closed dot, this is an adequate approach for our purposes, because we concentrate on the contribution to the peak spacing fluctuations coming from the non-zero conductance of the contacts. This contribution is determined by the randomness of the wave functions near the contacts. Fluctuating conductance peak heights, which depend on the same random quantity, apparently are well described by RMT.^{3,4}

In a partially open dot, the structure of the electron wave functions in the vicinity of the contacts affects both the amplitudes and positions of the conductance peaks. This results in a specific cross-correlation between these two characteristics of the random function $G(V_g)$. The correlation grows with the conductance of the contacts; we calculate the corresponding correlation function.

II. CONDUCTANCE PEAK POSITIONS

A. RMT Hamiltonian

In our consideration, the quantum dot is described by the Hamiltonian of the constant interaction model:

$$\hat{H}_0 = \sum_k \varepsilon_k c_k^\dagger c_k + \frac{E_C}{2} \left(\sum_k c_k^\dagger c_k - \mathcal{N} \right)^2. \quad (1)$$

In the framework of this model, the Coulomb repulsion of the electrons in the dot is accounted for by a relatively simple charging term [second term in (1)], and is characterized by only one parameter, namely, the “charging energy” of the dot, $E_C \equiv e^2/C$, where C is the total capacitance of the dot. The gate voltage V_g is represented by dimensionless parameter $\mathcal{N} \equiv C_g V_g/e$, with C_g being the capacitance of the dot with respect to the gate. The (random) one-electron spectrum in the dot is represented by the first term in Eq. (1), the energies ε_k are measured from the bottom of the band.

The weak dot-lead coupling can be accounted for by the tunneling Hamiltonian

$$\hat{H}_t = \sum_{k,p} \left(t_{kp} c_k^\dagger c_p + \text{H.c.} \right) + \sum_{k,q} \left(t_{kq} c_k^\dagger c_q + \text{H.c.} \right). \quad (2)$$

Here indices p and q denote the states in the left and right lead respectively. The dimensionless conductance of the dot-lead contacts is given by

$$g_L = (2\pi)^2 \langle |t_{kp}|^2 \rangle \frac{\nu_L}{\Delta}, \quad g_R = (2\pi)^2 \langle |t_{kq}|^2 \rangle \frac{\nu_R}{\Delta}, \quad (3)$$

where $\langle \dots \rangle$ denotes the averaging over a statistical ensemble, $\Delta \equiv \langle \varepsilon_{n+1} - \varepsilon_n \rangle$ is the average level spacing in the dot, and ν_α ($\alpha = L, R$) is the average density of states in the leads. A reflectionless dot-lead channel corresponds to $g = 1$; the conductance of such a channel equals G_0 ($G_0/2$ for spinless fermions).

The tunneling matrix elements are proportional to the values of the electron wave functions at the points \mathbf{r}_α of the dot-lead contacts. The randomness of the wave functions results in the fluctuations of the tunneling matrix elements in the Hamiltonian (2). The fluctuations of the wave functions in macroscopic leads can be neglected, and the tunneling matrix elements can be written in the form

$$t_{kp} = \frac{1}{2\pi} \sqrt{\frac{\Delta}{\nu_L}} \sqrt{g_L} \frac{\psi_k^*(\mathbf{r}_L)}{\sqrt{\langle \psi_k^2 \rangle}}, \quad t_{kq} = \frac{1}{2\pi} \sqrt{\frac{\Delta}{\nu_R}} \sqrt{g_R} \frac{\psi_k^*(\mathbf{r}_R)}{\sqrt{\langle \psi_k^2 \rangle}}. \quad (4)$$

In Sec. II B–II C we consider the model case of spinless fermions, which is easier to follow. The proper extension onto the case of real electrons with spins is performed in Sec. II D. Since at high temperatures the mesoscopic fluctuations are washed out, in this paper we concentrate on the low-temperature limit, $T < \Delta$.

B. Conductance peaks for spinless fermions

Near a Coulomb blockade peak, where conductance through the dot is mediated by one resonant level, the transmission coefficient of the dot at the Fermi level is given by the Breit-Wigner formula

$$\mathcal{T}(\mathcal{N}) = \frac{\Gamma_L \Gamma_R}{\epsilon(\mathcal{N})^2 + [(\Gamma_L + \Gamma_R)/2]^2}, \quad (5)$$

where Γ_α is the width of the resonant level with respect to electron tunneling to the α -th lead, and $\epsilon(\mathcal{N})$ is the deviation from the resonance. The center of the peak in the zero-bias conductance $G(\mathcal{N})$ for spinless fermions corresponds to such value of \mathcal{N} that $\epsilon = 0$.

For an almost isolated dot ($t_{kp}, t_{kq} \rightarrow 0$), function $\epsilon(\mathcal{N})$ near the n -th peak is given by

$$\epsilon = E_n^{(0)}(\mathcal{N}) - E_{n-1}^{(0)}(\mathcal{N}). \quad (6)$$

Here $E_n^{(0)}(\mathcal{N})$ is the ground state energy of an isolated dot with n particles [Hamiltonian (1)]. The values of \mathcal{N} , at which the conductance has a peak are thus determined by the equation

$$E_{n-1}^{(0)}(\mathcal{N}_n^{(0)}) = E_n^{(0)}(\mathcal{N}_n^{(0)}). \quad (7)$$

Therefore, for an almost isolated dot, when ϵ is given by Eq. (6), the spacing between the peaks is

$$\mathcal{U}_n^{(0)} \equiv \mathcal{N}_{n+1}^{(0)} - \mathcal{N}_n^{(0)} = 1 + \frac{\varepsilon_{n+1} - \varepsilon_n}{E_C}. \quad (8)$$

In this limit, the random component of the peak spacing has the same statistics as the level spacings $\Delta_n \equiv \varepsilon_{n+1} - \varepsilon_n$.

Upon the conductance increase, the electron transport through the dot is still dominated by the tunneling via the resonant level, as long as the effective level width remains small compared to the level spacing. The parameters entering in Eq. (5), however, acquire corrections due to the virtual processes involving other levels in the dot. The peak position is affected only by the corrections to ϵ . At weak dot-lead coupling, the latter can be evaluated in the second order of the perturbation theory in t_{kp}, t_{kq} , so ϵ is given by

$$\begin{aligned} \epsilon &= \left[E_n^{(0)}(\mathcal{N}) + \delta E_n'(\mathcal{N}) \right] \\ &\quad - \left[E_{n-1}^{(0)}(\mathcal{N}) + \delta E_{n-1}'(\mathcal{N}) \right], \quad (9) \\ \delta E_n'(\mathcal{N}) &= - \sum_p \left\{ \sum_{-\infty}^{k=n-1} \frac{|t_{kp}|^2 \theta(\xi_p)}{\xi_p + \varepsilon_n - \varepsilon_k + E_C(n - \mathcal{N} - 1/2)} \right. \\ &\quad \left. + \sum_{k=n+1}^{\infty} \frac{|t_{kp}|^2 \theta(-\xi_p)}{-\xi_p - \varepsilon_n + \varepsilon_k + E_C(\mathcal{N} - n + 3/2)} \right\} \\ &\quad - \sum_q \left\{ p \rightarrow q \right\}, \quad (10) \end{aligned}$$

where $\{p \rightarrow q\}$ denotes a term identical to the first term in braces in Eq. (10), but with all p 's replaced with q 's. Here $\delta E_n'$ is the correction to the energy of the state with n electrons in the dot due to the admixture of all the states with $n \pm 1$ electron, except for the lowest-energy state with $n - 1$ electrons. For spinless fermions, the mixing of the ground states with n and $n - 1$ particles in the dot determines the width of the n -th resonance (5) but does not affect its position. The equation for $\delta E_{n-1}'$ is similar to Eq. (10).

These corrections to ϵ shift the peak positions,

$$\mathcal{N}_n = \mathcal{N}_n^{(0)} + \delta \mathcal{N}_n'. \quad (11)$$

When the corrections $\delta E_n'(\mathcal{N})$ are small, the peak shifts $\delta \mathcal{N}_n'$ are also small and one can expand the right hand side of Eq. (9) in powers of $\delta \mathcal{N}$ in the vicinity of $\mathcal{N}_n^{(0)}$. Then it follows from Eqs. (1) and (9) that $\epsilon(\mathcal{N}) = 0$ when

$$\delta \mathcal{N}_n' = \frac{\delta E_n' - \delta E_{n-1}'}{\frac{\partial E_n^{(0)}}{\partial \mathcal{N}} - \frac{\partial E_{n-1}^{(0)}}{\partial \mathcal{N}}} \bigg|_{\mathcal{N}=\mathcal{N}_n^{(0)}} = \frac{\delta E_n' - \delta E_{n-1}'}{E_C} \bigg|_{\mathcal{N}=\mathcal{N}_n^{(0)}}. \quad (12)$$

Substituting the expressions for $\delta E_{n-1}'$ and $\delta E_n'$ [Eq. (10)] into Eq. (12), and using Eq. (4), we find the shift of the conductance peak resulting from the dot-lead coupling:

$$\begin{aligned} \delta \mathcal{N}_n' &= \frac{1}{(2\pi)^2} \frac{\Delta}{E_C} \left\{ \sum_{\alpha=L,R} \sum_k \text{sign}(\varepsilon_k - \varepsilon_n) g_\alpha \right. \\ &\quad \left. \times \frac{|\psi_k(\mathbf{r}_\alpha)|^2}{\langle |\psi_k|^2 \rangle} \ln \frac{E_C + |\varepsilon_n - \varepsilon_k|}{|\varepsilon_n - \varepsilon_k|} \right\}. \quad (13) \end{aligned}$$

The ensemble average of this shift equals zero. However, the mesoscopic fluctuations of the wave functions in the dot result in non-zero random shifts of the conductance peaks in each particular realization. Equation (13) yields the following expression for the fluctuating component of the spacing between the n th and $(n + 1)$ st conductance peaks:

$$\mathcal{U}_n = \mathcal{U}_n^{(0)} + \delta \mathcal{U}_n', \quad (14)$$

$$\begin{aligned} \delta \mathcal{U}_n' &\equiv \delta \mathcal{N}_{n+1}' - \delta \mathcal{N}_n' \\ &= \frac{\Delta}{E_C} \sum_{\substack{\alpha=L,R \\ l=n,n+1}} \gamma'_\alpha \left(1 - \frac{|\psi_l(\mathbf{r}_\alpha)|^2}{\langle |\psi_l|^2 \rangle} \right), \quad (15) \end{aligned}$$

where

$$\gamma'_\alpha = \frac{1}{(2\pi)^2} g_\alpha \ln \frac{E_C}{\Delta}. \quad (16)$$

The term $\delta \mathcal{U}_n'$ in Eq. (14) describes the contribution of the dot-lead coupling to the fluctuations of the spacing between the Coulomb blockade peaks. This contribution is statistically independent of the term $\mathcal{U}_n^{(0)}$, which accounts for the fluctuations in the energy spectrum of the dot and is given by Eq. (8). The logarithmic factor in Eq. (16) is the result of summation over the lead states between the effective upper and lower cut-offs, E_C and Δ . The contributions of the wave functions of the states other than n and $n + 1$ do not contain the large factor $\ln(E_C/\Delta)$ and are neglected.

C. Spinless fermions: renormalization group approach

Let us discuss the region of applicability of Eqs. (15)–(16). The right-hand side of Eq. (16), obtained in the lowest non-vanishing order of the perturbation theory in t_{kp} , t_{kq} , is proportional to the product of the small parameter g_α and the large factor $\ln(E_C/\Delta)$. Examination of the higher orders of the perturbation theory shows that the leading term of the m th order is proportional to

$$\frac{\Delta}{E_C} \sqrt{g_\alpha} \left[\sqrt{g_\alpha} \ln \frac{E_C}{\Delta} \right]^m. \quad (17)$$

Thus the results presented by Eqs. (15)–(16) are valid only if the condition

$$\sqrt{g_\alpha} \ln \frac{E_C}{\Delta} \ll 1 \quad (18)$$

is satisfied. However, beyond the limits of the applicability of the finite order perturbation theory, which are given by Eq. (18), one can exploit the leading logarithm approximation. It consists in summation of the leading terms [see Eq. (17)] of all orders of the perturbation theory. This can be done by means of the same renormalization group technique, which was initially developed by Anderson for the Kondo problem.¹¹ Application of this method to the Coulomb blockade problem¹² allows one to obtain results in the domain of parameters

$$\sqrt{g_\alpha} \ln \frac{E_C}{\Delta} \lesssim 1, \quad (19)$$

which is wider than the region of applicability (18) of the finite order perturbation theory. The technique used in Ref. 12, as well as the original technique by Anderson, does not account for the mesoscopic fluctuations of the one-electron wave functions. For our purposes, we need to extend the renormalization group method to account for the randomness of the electron states in the dot. Below we present the proper generalization valid for a dot obeying the RMT statistics.

The Anderson's scaling procedure consists in transformation of the initial Hamiltonian $\hat{H}_0 + \hat{H}_t$ to a new one, with smaller bandwidth and with the matrix elements renormalized to compensate for this band reduction. The transformation operates within the invariant space of Hamiltonians having generic form

$$\sum_j \left[\mathbf{E}_0^{(j)} + \sum_{\eta_1 \eta_2} \mathbf{T}_{\eta_1 \eta_2}^{(j)} c_{\eta_1}^\dagger c_{\eta_2} \right] \hat{P}_j, \quad (20)$$

where the indices η_1, η_2 run through the one-particle states in the dot and both leads, and \hat{P}_j is the operator of projection to the Hilbert subspace of states with j particles in the dot. Near the n -th peak, the renormalization of the Hamiltonian occurs mostly due to the virtual transitions between the states with n and $n-1$

particles in the dot, and it is sufficient to limit our consideration to these two sets of states. Then the summation in Eq. (20) must be done over $j = n-1, n$ only, and $\mathbf{T}_{kp}^{(n)}, \mathbf{T}_{pk}^{(n-1)}, \mathbf{T}_{kq}^{(n)}, \mathbf{T}_{qk}^{(n-1)} \equiv 0$ because the corresponding transitions involve states outside this subspace of states.

The transformation starts from Hamiltonian (1)–(2) operating within the electron band of width $D_0 \sim E_C$. In the course of renormalization, the band width D is reduced in steps starting from $D = D_0$. As we mentioned above, the matrix elements must be adjusted to compensate for the band reduction: after each step, the transition amplitudes calculated with the renormalized Hamiltonian $\hat{H}(D - dD)$ must coincide with those derived from the Hamiltonian $\hat{H}(D)$ of the previous step. In the leading logarithmic approximation, which we employ, these amplitudes should be calculated in the second order of the perturbation theory. Then the scaling law, which dictates how a matrix element must be changed when the bandwidth is reduced from D to $D - dD$, in general reads

$$d\mathbf{T}_{\eta_1 \eta_2}^{(j)} = \sum_{D-dD < |\xi_{\eta_3}| < D} \frac{\mathbf{T}_{\eta_1 \eta_3}^{(j_3)} \mathbf{T}_{\eta_3 \eta_2}^{(j)}}{-\mathcal{E}[\eta_2 \rightarrow \eta_3]}, \quad (21)$$

where $\mathcal{E}[\eta_2 \rightarrow \eta_3]$ is the energy difference associated with the (virtual) transition $\eta_2 \rightarrow \eta_3$, and j_3 is the number of electrons in the dot after this transition. Here we present explicitly only the equation for $\mathbf{T}_{k_1 k_2}^{(n)}$:

$$\begin{aligned} d\mathbf{T}_{k_1 k_2}^{(n)} = & \sum_{-D < \xi_p < -D+dD} \frac{\mathbf{T}_{k_1 p} \mathbf{T}_{p k_2}}{D} + \sum_{-D < \xi_q < -D+dD} \frac{\mathbf{T}_{k_1 q} \mathbf{T}_{q k_2}}{D} \\ & - \sum_{D-dD < \xi_{k_3} < D} \frac{\mathbf{T}_{k_1 k_3}^{(n)} \mathbf{T}_{k_3 k_2}^{(n)}}{D} + \sum_{-D < \xi_{k_3} < -D+dD} \frac{\mathbf{T}_{k_1 k_3}^{(n)} \mathbf{T}_{k_3 k_2}^{(n)}}{D}. \end{aligned} \quad (22)$$

The equations for the other parameters of the Hamiltonian have similar form. The renormalization procedure also generates the constant term \mathbf{E}_0 :

$$d\mathbf{E}_0^{(j)} = - \sum_{\substack{-D < \xi_{\eta_1} < -D+dD \\ D-dD < \xi_{\eta_2} < D}} \frac{\mathbf{T}_{\eta_2 \eta_1}^{(j_1)} \mathbf{T}_{\eta_1 \eta_2}^{(j)}}{2D} + \sum_{-D < \xi_\eta < -D+dD} \mathbf{T}_{\eta \eta}^{(j)}. \quad (23)$$

The initial Hamiltonian $\hat{H}(D = E_C) \equiv \hat{H}_0 + \hat{H}_t$ [Eqs. (1)–(2)] in terms of Eq. (20) with $j = n-1, n$ corresponds to

$$\begin{aligned} \mathbf{E}_0^{(j)} &= 0, \\ \mathbf{T}_{kp} &\equiv \mathbf{T}_{pk}^* = t_{kp}, \quad \mathbf{T}_{kq} \equiv \mathbf{T}_{qk}^* = t_{kq}, \\ \mathbf{T}_{k_1 k_2}^{(j)} &= 0, \quad \mathbf{T}_{p_1 p_2}^{(j)} = 0, \quad \mathbf{T}_{q_1 q_2}^{(j)} = 0. \end{aligned} \quad (24)$$

It is random because of the fluctuations of one-electron wave functions [see Eq. (4)] and level spacings. The

Hamiltonian $\hat{H}(D < E_C)$, which is produced by the scaling transformation from $\hat{H}_0 + \hat{H}_t$, is therefore also random.

As it can be seen from Eq. (22), the randomness of the initial Hamiltonian $\hat{H}_0 + \hat{H}_t$ is inherited by the renormalized Hamiltonian $\hat{H}(D)$ in two ways. First, there are random contributions from the states k_1 and k_2 . Second, there are also random contributions from the states k_3 , being eliminated by the band reduction. The final renormalized matrix element $T_{k_1 k_2}$ will still be proportional to the (random) wave functions $\psi_{k_1}^*$ and ψ_{k_2} . On the contrary, the random contributions from the eliminated states k_3 are added together and their (independent) fluctuations are averaged out. This consideration leads one to the conclusion that the solutions of the RG equations (21) can be cast in the form:

$$T_{k_1 k_2}^{(j)}(D) = \pm \Delta \sum_{\alpha=L,R} \frac{\psi_{k_1}^*(\mathbf{r}_\alpha) \psi_{k_2}(\mathbf{r}_\alpha)}{\langle \psi_k^2 \rangle} \lambda_\alpha(D), \quad (25a)$$

$$T_{kp}(D) = \sqrt{\frac{\Delta}{\nu_L}} \frac{\psi_k(\mathbf{r}_L)}{\sqrt{\langle \psi_k^2 \rangle}} \mu_L(D), \quad (25b)$$

$$T_{kq}(D) = \sqrt{\frac{\Delta}{\nu_R}} \frac{\psi_k(\mathbf{r}_R)}{\sqrt{\langle \psi_k^2 \rangle}} \mu_R(D), \quad (25c)$$

$$T_{p_1 p_2}^{(j)}(D) = \mp \frac{1}{\nu_L} \lambda_L(D). \quad (25d)$$

$$T_{q_1 q_2}^{(j)}(D) = \mp \frac{1}{\nu_R} \lambda_R(D). \quad (25e)$$

Here the upper sign in the right-hand-sides corresponds to $j = n - 1$ and the lower sign corresponds to $j = n$. From Eqs. (21), (24), and (25), we derive the scaling equations for the non-fluctuating parameters λ_i and μ_i , which determine the behavior of the Hamiltonian in the course of the scaling procedure:

$$\frac{d\lambda_\alpha(D)}{d \ln D} = \mu_\alpha^2(D), \quad \frac{d\mu_\alpha(D)}{d \ln D} = 4\lambda_\alpha(D)\mu_\alpha(D) \quad (26)$$

with the initial conditions

$$\lambda_\alpha(D = E_C) = 0, \quad \mu_\alpha(D = E_C) = \frac{1}{2\pi} \sqrt{g_\alpha}. \quad (27)$$

They coincide with those derived in Ref. 12 and have solutions

$$\lambda_\alpha(D) = \frac{1}{4\pi} \sqrt{g_\alpha} \tan \left[\frac{1}{\pi} \sqrt{g_\alpha} \ln \frac{E_C}{D} \right],$$

$$\mu_\alpha(D) = \frac{1}{2\pi} \sqrt{g_\alpha} \left\{ \cos \left[\frac{1}{\pi} \sqrt{g_\alpha} \ln \frac{E_C}{D} \right] \right\}^{-1}. \quad (28)$$

The energy shift E_0 also accumulates in the course of renormalization. Its random part, which stems from the fluctuations of the wave functions of the eliminated states k_3 , averages out due to the summation over a large number of these intermediate states, similarly to the corresponding contribution to the matrix elements $T_{p_1 p_2}$ and $T_{q_1 q_2}$.

The transformation can proceed until the band width is reduced to the value of the order of the mean level spacing Δ . After the renormalization, the ground state energy can be found with the help of Hamiltonian $\hat{H}(D \sim \Delta)$ as the sum of E_0 and the correction due to the dot-lead tunneling in the reduced band. As we explained above, the latter term is the main source of fluctuations of the ground state energy. It can be calculated in the second order of the perturbation theory in $T_{\eta_1 \eta_2}$, similarly to Eq. (10). This calculation finally yields Eq. (15) with

$$\gamma'_\alpha = \frac{1}{4\pi} \sqrt{g_\alpha} \tan \left[\frac{1}{\pi} \sqrt{g_\alpha} \ln \frac{E_C}{\Delta} \right]. \quad (29)$$

If the argument of the tangent function is much less than unity, Eq. (29) is reduced to Eq. (16), as expected.

D. Electrons with spin

In this section we will refer to the same Hamiltonian (1)–(2), with summation over the spin index added. The conductance peaks are numbered as follows: the $(2m-1)$ -th conductance peak corresponds to the resonant tunneling of an electron through the empty m -th level, and the $(2m)$ -th peak corresponds to resonant electron tunneling via the m -th level already occupied by one electron.

In principle, the spin degeneracy can lead to formation of the many-body state, which enhances the conductance in the valley between the $(2m-1)$ -th and $(2m)$ -th peaks, so Eq. (5) is no longer valid. This phenomenon is commonly referred to as the Kondo effect. However if the temperature is larger than the widths of the dot levels, which is the case under consideration, the formation of this many-body state is suppressed, and we can employ the rate equation formalism to evaluate the conductance of the dot. This approach yields the following expression for the dot conductance:¹³

$$G(\mathcal{N}) = G_0 \frac{g_L g_R}{g_L + g_R} \frac{\partial f_F[\epsilon(\mathcal{N})]/\partial \epsilon}{1 + f_F[\pm \epsilon(\mathcal{N})]}, \quad (30)$$

where $f_F(\xi) \equiv 1/[\exp(\xi/T) + 1]$ is the Fermi distribution function. The sign in the denominator should be taken “+” for even peaks and “−” for odd peaks. One can see that the peaks in the conductance $G(\mathcal{N})$ are shifted from the points of charge degeneracy, which correspond to $\epsilon(\mathcal{N}) = 0$, by $\pm(\ln 2/2)T$, which results in the correction to the peak spacings:

$$\delta \mathcal{U}_{2m-1}^{(T)} = (\ln 2) \frac{T}{E_C}, \quad \delta \mathcal{U}_{2m}^{(T)} = -(\ln 2) \frac{T}{E_C}. \quad (31)$$

For an almost isolated dot, the distances between the charge degeneracy points are given by

$$\mathcal{U}_{2m-1}^{(0)} = 1, \quad (32a)$$

$$\mathcal{U}_{2m}^{(0)} = 1 + \frac{\varepsilon_{m+1} - \varepsilon_m}{E_C}. \quad (32b)$$

To obtain the expressions for the conductance peak spacings for a partially open dot, one has to add up $\mathcal{U}^{(0)}$, $\delta\mathcal{U}^{(T)}$, and the contribution to the peak spacing due to the finite dot-lead tunneling. This contribution has two components.

The first component, $\delta\mathcal{U}'_n$, is analogous to the one calculated in Sec. II B, it comes from the transitions involving all levels in the dot except for the resonant one. The spacing \mathcal{U}_{2m} is between the conductance peaks corresponding to filling of two consecutive orbital levels. The result for spinless fermions is given by Eq. (15). For electrons with spin the corresponding correction acquires an additional factor of 2:

$$\delta\mathcal{U}'_{2m} = 2 \frac{\Delta}{E_C} \sum_{\substack{\alpha=L,R \\ l=m,m+1}} \gamma'_\alpha \left(1 - \frac{|\psi_l(\mathbf{r}_\alpha)|^2}{\langle |\psi_l|^2 \rangle} \right). \quad (33a)$$

The correction of this type contribute equally to the positions \mathcal{N}_{2m-1} , \mathcal{N}_{2m} or the peaks, corresponding to the same orbital level. As the result

$$\delta\mathcal{U}'_{2m-1} = 0. \quad (33b)$$

The other component, $\delta\mathcal{U}''_n$, is due to the virtual transitions from/to the resonant level. Let us consider, for definiteness, the $2m$ -th conductance peak, whose position is determined by the energies of the ground states $|2m-1\rangle$ and $|2m\rangle$, with $2m-1$ and $2m$ electrons in the dot respectively. For spinless fermions, virtual transitions involving the m -th level do not lead to the shift of the peak position, because of the electron-hole symmetry. The spin degeneracy, however, removes this symmetry and as the result the shifts of the ground state energies δE_{2m} and δE_{2m-1} are not equal.¹⁴ The state $|2m\rangle$ acquires an admixture of the excited states with $2m-1$ electrons in the dot, and the corresponding correction is given by

$$\delta E''_{2m} = -2 \left[\sum_p \frac{|t_{mp}|^2 \theta(\xi_p)}{\xi_p} + \sum_q \frac{|t_{mq}|^2 \theta(\xi_q)}{\xi_q} \right], \quad (34a)$$

where the prefactor 2 is due to the spin degeneracy. The state $|2m-1\rangle$ intermixes with the excited states having $2m$ or $2m-2$ electrons in the dot. At the point of the $2m$ -th conductance peak, which we consider, the states $|2m-1\rangle$ and $|2m\rangle$ have equal energy, but the energy of the state $|2m-2\rangle$ is higher, because of the charging. Therefore the coupling of the states with $2m-1$ and $2m-2$ electrons in the dot is suppressed and the correction $\delta E''_{2m-1}$ is smaller than $\delta E''_{2m}$:

$$\begin{aligned} \delta E''_{2m-1} = & - \left[\sum_p \frac{|t_{mp}|^2 \theta(-\xi_p)}{-\xi_p} + \sum_p \frac{|t_{mp}|^2 \theta(\xi_p)}{\xi_p + 2E_C} \right] \\ & - \left[p \rightarrow q \right]. \end{aligned} \quad (34b)$$

Substitution of Eqs. (34) into Eq. (12) yields

$$\delta\mathcal{N}''_{2m} = -\frac{\Delta}{E_C} \sum_{\alpha=L,R} \gamma''_\alpha \frac{|\psi_m(\mathbf{r}_\alpha)|^2}{\langle |\psi_m|^2 \rangle}, \quad (35)$$

with

$$\gamma''_\alpha = \frac{1}{(2\pi)^2} g_\alpha \ln \frac{E_C}{T}. \quad (36)$$

The shift of an odd peak can be calculated analogously and is given by

$$\delta\mathcal{N}''_{2m-1} = -\delta\mathcal{N}''_{2m}. \quad (37)$$

In contrast to the correction from the non-resonant levels [Eq. (12)], the correction $\delta\mathcal{N}''_n$ has a non-zero ensemble average,

$$\langle \delta\mathcal{N}''_n \rangle = (-1)^{n-1} \sum_{\alpha=L,R} \gamma''_\alpha \frac{\Delta}{E_C}. \quad (38)$$

Equations (35), (37) yield

$$\delta\mathcal{U}''_{2m} = \frac{\Delta}{E_C} \sum_{\substack{\alpha=L,R \\ l=m,m+1}} \gamma''_\alpha \frac{|\psi_l(\mathbf{r}_\alpha)|^2}{\langle |\psi_l|^2 \rangle}, \quad (39a)$$

$$\delta\mathcal{U}''_{2m-1} = -2 \frac{\Delta}{E_C} \sum_{\alpha=L,R} \gamma''_\alpha \frac{|\psi_m(\mathbf{r}_\alpha)|^2}{\langle |\psi_m|^2 \rangle}. \quad (39b)$$

The full expression for the peak spacings in the case of electrons with spin is

$$\mathcal{U}_n = \mathcal{U}_n^{(0)} + \delta\mathcal{U}_n^{(T)} + \delta\mathcal{U}'_n + \delta\mathcal{U}''_n, \quad (40)$$

where $\delta\mathcal{U}_n^{(T)}$ and $\mathcal{U}_n^{(0)}$ are given by Eqs. (31) and (32) respectively.

Equations (35)-(36), derived with the help of the second order perturbation theory in t_{kp} , t_{kq} , are valid only at relatively small values of the conductances g_α of the contacts (see Sec. II C). When the perturbation theory fails, the proper expression for γ''_α can be obtained with the help of the renormalization group method, described in Sec. II C. If the temperature is of the order of the mean level spacing, then the RG transformation must be stopped when the bandwidth D is reduced to Δ ; the renormalized γ''_α equals γ'_α , which is given by Eq. (29).

If $T < \Delta$, then we have to continue the renormalization procedure to the bandwidths $D < \Delta$. There is only one level in the dot within such a band, so Eqs. (21), (25) yield:

$$\frac{d\lambda_\alpha(D)}{d \ln D} = \mu_\alpha^2(D), \quad \frac{d\mu_\alpha(D)}{d \ln D} = 2\mu_\alpha(D)\lambda_\alpha(\Delta). \quad (41)$$

The solutions of these equations determine the renormalization of the tunneling matrix elements $T_{k_1 k_2}$, T_{kp} , and T_{kq} given by Eqs. (25a)–(25c). As for $T_{p_1 p_2}$ and $T_{q_1 q_2}$, they are not renormalized anymore and are given by Eqs. (25d)–(25e) with $D = \Delta$. The renormalization procedure should be carried out until $D \sim T$. Finally we extend our result (35) to a wider region of parameters, defined by Eq. (19), with parameter γ''_α given by

$$\gamma''_\alpha = \gamma'_\alpha + \frac{\mu_\alpha^2(\Delta)}{2\lambda_\alpha(\Delta)} \left[\left(\frac{\Delta}{T} \right)^{2\lambda_\alpha(\Delta)} - 1 \right]. \quad (42)$$

Here $\lambda_\alpha(\Delta)$ and $\mu_\alpha(\Delta)$ are determined by Eqs. (28). The first term in Eq. (42) is produced in the course of renormalization while the band is reduced to Δ ; the second term is produced by the band reduction from Δ to T . Like in the spinless case, Eq. (42) reduces to Eq. (36) at small values of the dot-lead conductance, *i.e.* when the condition (18) is satisfied.

III. STATISTICAL PROPERTIES OF THE PEAK SPACING

A. Peak spacing fluctuations

Now we discuss how the finite tunneling strength affects the distribution function of the peak spacings, which is given by

$$P_n(\mathcal{U}) = \int d\mathcal{U}_n^{(0)} P^{(0)}(\mathcal{U}_n^{(0)}) \prod_{\alpha=L,R} d\{\psi\}(\mathbf{r}_\alpha) P(\{\psi\}(\mathbf{r}_\alpha)) \times \delta(\mathcal{U} - \mathcal{U}_n). \quad (43)$$

Here \mathcal{U}_n is determined by Eq. (40). It follows from Eq. (32) that the distribution function of $\mathcal{U}_n^{(0)}$, $P^{(0)}$, is a δ -function for $n = 2m - 1$, and is given by the Wigner-Dyson distribution function for $n = 2m$. The set $\{\psi\}$ denotes the wave functions entering Eqs. (33) and (39) for $\delta\mathcal{U}'_n$ and $\delta\mathcal{U}''_n$. The values $\psi_m(\mathbf{r})$ are distributed according to the Porter-Thomas statistics.

At small junction conductance, corrections $\delta\mathcal{U}'_n$, $\delta\mathcal{U}''_n$ are negligible. In this limit, the distribution of the peak spacings is manifestly bimodal. Odd values of n correspond to the spacing between two peaks originating from filling of the same orbital level in the dot; the corresponding distribution function is infinitely sharp, and is centered at $\mathcal{U} = 1 + T \ln 2 / E_C$. Peak spacings at even n correspond to filling of the consecutive orbital levels, and therefore the distribution function for them follows the Wigner-Dyson statistics. Note, that at a finite temperature the centers of the “even” and “odd” distributions are shifted towards each other, so these two distributions overlap. This shift, which is the result of interaction between the electrons tunneling via a spin-degenerate level, was not taken into account in the analysis of experimental data.⁷

At finite contact conductance, mesoscopic fluctuations of the wave functions in the dot yield a finite width of the “odd” distribution and broaden the “even” distribution. These effects stem from a finite value of $\delta\mathcal{U}'_n$ and $\delta\mathcal{U}''_n$. The resulting widths are characterized by

$$\langle (\delta\mathcal{U}_{2m-1})^2 \rangle = \frac{8}{\beta} \sum_{\alpha=L,R} (\gamma''_\alpha)^2 \left(\frac{\Delta}{E_C} \right)^2, \quad (44a)$$

$$\langle (\delta\mathcal{U}_{2m})^2 \rangle = \frac{4}{\beta} \sum_{\alpha=L,R} (2\gamma'_\alpha - \gamma''_\alpha)^2 \left(\frac{\Delta}{E_C} \right)^2 + \frac{\langle \delta\Delta_n^2 \rangle}{E_C^2}. \quad (44b)$$

Here $\beta = 1$ and 2 for orthogonal and unitary ensembles respectively. For smaller values of junction conductances g_α [such that condition (18) is satisfied], γ'_α and γ''_α are proportional to g_α and are given by Eqs. (16) and (36) respectively. Larger conductances cause renormalization of γ'_α and γ''_α ; the resulting expressions for them are given by Eqs. (29) and (42).

One can see from Eq. (44b) that there are two independent additive contributions to the fluctuations of the peak spacing. The first one is due to the fluctuations of the wave functions and is proportional to the junction conductance. The second one comes from the fluctuations of the electron spectrum. If the latter is described by RMT, then $\langle \delta\Delta_n^2 \rangle = [(4/\pi) - 1]\Delta^2$ and $\langle \delta\Delta_n^2 \rangle = [(3\pi/8) - 1]\Delta^2$ for orthogonal and unitary ensembles respectively. The experimentally measured⁷ $\langle \delta\Delta_n^2 \rangle$ apparently are larger than the values predicted by RMT. Regardless this discrepancy, the contribution coming from the randomness of the wave functions can be singled out from experimental data by comparing the values of $\langle \delta\mathcal{U}_n^2 \rangle$ measured at various junction conductances.

The average spacing between the peaks is also affected by finite conductance:

$$\langle \mathcal{U}_{2m-1} \rangle = 1 + (\ln 2) \frac{T}{E_C} - 2 \sum_{\alpha=L,R} \gamma''_\alpha \frac{\Delta}{E_C}, \quad (45a)$$

$$\langle \mathcal{U}_{2m} \rangle = 1 + \frac{\Delta}{E_C} - (\ln 2) \frac{T}{E_C} + 2 \sum_{\alpha=L,R} \gamma''_\alpha \frac{\Delta}{E_C}. \quad (45b)$$

One can also consider the distribution function averaged over even and odd peak spacings. A sample plot of this function is shown in Fig. 1. It is instructive, following the experimental paper,⁷ to compare this function to the distribution function $P^{(0)}(\mathcal{U})$ of the spacings between the charge degeneracy points in an almost isolated dot. The “bimodal” distribution $P^{(0)}(\mathcal{U})$ consists of the Wigner-Dyson distribution (“even” spacings) and a δ -peak (“odd” spacings). The key differences of $P(\mathcal{U})$ from $P^{(0)}(\mathcal{U})$ are as follows: (i) the δ -peak corresponding to odd spacings is broadened (ii) the centers of the distribution maxima corresponding to even and odd peak spacings are shifted by $\pm[(\ln 2)T/E_C - 2(\sum_\alpha \gamma''_\alpha)\Delta/E_C]$

(iii) unlike $P^{(0)}(\mathcal{U})$, the distribution $P(\mathcal{U})$ has a tail which extends into the region $\mathcal{U} < 1$.

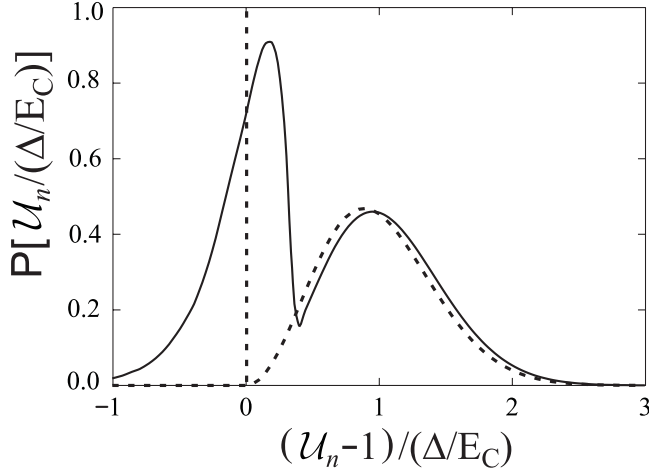


FIG. 1. The cumulative distribution function of the “even” and “odd” spacings between the Coulomb blockade peaks, $\mathcal{U}_n/(\Delta/E_C)$, given by Eqs. (33), (39) for $\gamma'_\alpha = 0.075$, $\gamma''_\alpha = 0.1$, $T = 0.5\Delta$ (solid line). The dotted line shows the “bimodal” distribution $P^{(0)}$ consisting of the Wigner-Dyson distribution (“even” spacings) and a δ -peak (“odd” spacings). The shown distributions correspond to the Gaussian unitary ensemble.

One can see from Eq. (44) that the fluctuations of wave functions and of the level spacings contribute equally to the width of $P(\mathcal{U})$ at $\gamma'_\alpha \sim \gamma''_\alpha \sim 0.15$. The dimensionless parameters γ'_α and γ''_α depend not only on the junction conductances, but also on the ratios E_C/Δ and E_C/T , see Eqs. (29) and (42). Using the values $E_C = 300\mu\text{eV}$, $\Delta = 7\mu\text{eV}$, and $T \sim \Delta$ from the experiment of Ref. 7, we obtain that the values $\gamma'_\alpha \sim 0.05$ are reached when the junction conductances equal to $0.5G_0$. Thus a considerable contribution of wave function fluctuations to the randomness of the interpeak spacings can be achieved when the conductance peaks are still well-defined.

B. Correlations between the heights of the peaks and their spacings

We have shown that for a partially open dot, the conductance peak positions depend on the values of the one-electron wave functions at the points of the dot-lead contacts. On the other hand, these values determine also the conductance peak amplitudes:

$$G_{2m-1}^{(\max)} = G_{2m}^{(\max)} \propto \frac{g_L |\psi_m(\mathbf{r}_L)|^2 g_R |\psi_m(\mathbf{r}_R)|^2}{g_L |\psi_m(\mathbf{r}_L)|^2 + g_R |\psi_m(\mathbf{r}_R)|^2}. \quad (46)$$

Therefore the spacing between two peaks must be correlated with the heights of these peaks: the higher the peaks are, the less (on average) is the spacing between them.

The joint distribution function of the conductance peak height $G^{(\max)}$ and the spacing of this peak from its neighbors $\tilde{\mathcal{U}}$ is given by

$$P(\tilde{\mathcal{U}}, G^{(\max)}) = \int d\mathcal{U}_n^{(0)} P^{(0)}(\mathcal{U}_n^{(0)}) \times \prod_{\alpha=L,R} d\{\psi\}(\mathbf{r}_\alpha) P(\{\psi\}(\mathbf{r}_\alpha)) \times \delta(\tilde{\mathcal{U}} - \tilde{\mathcal{U}}_n) \delta(G^{(\max)} - G_n^{(\max)}). \quad (47)$$

Here the spacing of the n -th peak from its neighbors is

$$\tilde{\mathcal{U}}_n \equiv \frac{\mathcal{U}_n + \mathcal{U}_{n+1}}{2},$$

and \mathcal{U}_n is given by Eq. (40). The distribution $P(\tilde{\mathcal{U}}, G^{(\max)})$ is skewed, *i.e.* $\langle \delta\tilde{\mathcal{U}} \delta G^{(\max)} \rangle \neq 0$, because of the dependence of $\tilde{\mathcal{U}}$ on $\{\psi\}$. The dimensionless cross-correlation parameter grows with junction conductance,

$$K_{G-\mathcal{U}} \equiv \frac{\langle \delta G_n^{(\max)} \delta \tilde{\mathcal{U}}_n \rangle}{\langle G_n^{(\max)} \rangle \langle \Delta/E_C \rangle} = - \sum_{\substack{\alpha=L,R \\ \alpha' \neq \alpha}} \mathcal{F}\left(\frac{g_{\alpha'}}{g_\alpha}\right) (2\gamma'_\alpha + \gamma''_\alpha). \quad (48)$$

Function $\mathcal{F}(x) > 0$ is given by

$$\mathcal{F}(x) = \frac{2\sqrt{x}}{1 + \sqrt{x}}$$

for the orthogonal ensemble and by

$$\mathcal{F}(x) = \frac{2x^3 + 3x^2 - 6x + 1 - 6x^2 \ln x}{(x-1)(x^2 - 1 - 2x \ln x)} - 1$$

for the unitary ensemble. In the case $g_L = g_R$, the argument of the function \mathcal{F} in Eq. (48) equals unity; $\mathcal{F}(1) = 1$ and $3/2$ for the orthogonal and unitary ensemble respectively.

C. Fluctuations of spacing between distant peaks

In the previous sections we considered only the fluctuations of spacing between the neighboring peaks. Now we will discuss the statistical properties of the spacing between the n -th and $(n+l)$ -th peaks,

$$\mathcal{U}_n(l) \equiv \mathcal{N}_{n+l} - \mathcal{N}_n, \quad (49)$$

with $l > 1$. Here we must mention that in real dots adding electrons apparently scrambles the one-electron states.¹⁵ However, according to the experiment,^{10,15} the changes in the dot's one-electron spectrum and wave functions are small when the number of added electrons is small. Under these conditions, the same realization of the random parameters of the Hamiltonian (1)-(2) determines the positions of n th and $(n+l)$ th peaks. The

average spacing between the peaks can be derived from Eqs. (31), (32) and (38), and is given by

$$\langle \mathcal{U}_n(l) \rangle = l \left(1 + \frac{\Delta}{2E_C} \right) + [(-1)^{n+l} - (-1)^n] \times \frac{\Delta}{E_C} \left[-\frac{1}{2} + \frac{\ln 2}{2} \frac{T}{\Delta} - \sum_{\alpha=L,R} \gamma''_{\alpha} \right]. \quad (50)$$

Like in the case of neighboring peaks, which we considered in Sec. II, the fluctuations of the peak spacings have the independent contributions $\delta \mathcal{U}'$, $\delta \mathcal{U}''$ and $\mathcal{U}^{(0)}$ coming from the randomness of the wave functions and level spacings respectively. Using Eqs. (13), (31) and (35), we obtain for $l \ll E_C/\Delta$

$$\langle [\delta \mathcal{U}'_n(l) + \delta \mathcal{U}''_n(l)]^2 \rangle = \frac{4}{\beta} \left(\frac{\Delta}{E_C} \right)^2 \times \sum_{\alpha=L,R} [4(l-1)(\gamma'_{\alpha})^2 + B_{\alpha}], \quad (51)$$

where B_{α} depend only on whether the numbers n and $n+l$ are even or odd, and do not grow with l :

$$B_{\alpha} = \begin{cases} (\gamma''_{\alpha})^2 & \text{even } l, \\ (2\gamma'_{\alpha} + \gamma''_{\alpha})^2 - 8(\gamma'_{\alpha})^2, & \text{odd } l \geq 3, \text{ odd } n, \\ (\gamma''_{\alpha})^2, & l = 1, \text{ odd } n, \\ (2\gamma'_{\alpha} - \gamma''_{\alpha})^2, & \text{odd } l, \text{ even } n. \end{cases}$$

Thus the contribution due to the fluctuations of the wave functions, $\delta \mathcal{U}'_n(l) + \delta \mathcal{U}''_n(l)$, is proportional to the junction conductance, and its variance grows linearly with the distance l between the peaks. This behavior is in qualitative agreement with the experiments.¹⁰ The fluctuations of the other contribution, $\delta \mathcal{U}_n^{(0)}(l)$, do not depend on the junction conductance, and are characterized by

$$\langle [\delta \mathcal{U}_n^{(0)}(l)]^2 \rangle = \left(\frac{\Delta}{E_C} \right)^2 F \left(\frac{l + (-1)^{n+l} - (-1)^n}{2} \right). \quad (52)$$

Function $F(k)$ determines the variance of the spacing between two distant one-electron energy levels, and is given by the RMT; $F(k) \sim \ln k$ at $k \gg 1$. One can see that for sufficiently distant peaks and large junction conductances, $\delta \mathcal{U}'(l) + \delta \mathcal{U}''(l)$ dominates over $\delta \mathcal{U}^{(0)}(l)$, and the main term in the fluctuations of the spacing comes from the fluctuations of the wave functions at the points of dot-lead contacts.

At large l , the correlations between the sets of the levels that determine the shifts of the n -th and $(n+l)$ -th peaks become negligible. If the Hamiltonian of the dot is not affected by adding of new electrons, it occurs at $l \sim E_C/\Delta$, when these two sets of levels, having characteristic width E_C each, no more overlap. In real dots, it can occur even at smaller l , because by adding electrons one modifies the effective potential which confines

electrons to the dot. Eventually the modifications result in a loss of correlations between the one-electron states in the original and new potentials. Then the positions of distant peaks are defined by two Hamiltonians, both of the generic form (1)-(2) with the same E_C , but with different and statistically independent (random) t_{kp} , t_{kq} and ε_k . The resulting variance of the peak spacing at large l is twice the variance of a peak position [Eq. (12)] and is given by

$$\langle [\delta \mathcal{U}'_n(l)]^2 \rangle = \frac{1}{6\pi^2\beta} \frac{\Delta}{E_C} \sum_{\alpha=L,R} g_{\alpha}^2. \quad (53)$$

The contribution $\delta \mathcal{U}''_n(l)$ does not grow with l and is neglected here.

Thus the fluctuations of the interpeak spacing due to randomness of the wave functions saturate at large distances between the peaks. The corresponding fluctuation amplitude exceeds that for the neighboring peaks by a parametrically large factor $\sqrt{E_C/\Delta}/[\ln(E_C/\Delta)]^2$. This saturation of the peak spacing fluctuations with the increase of l is in agreement with the experimental results (see Fig. 2 in Ref. 10).

As for the contribution of the level spacing fluctuations, $\mathcal{U}_n^{(0)}(l)$, its statistical properties for large l depend crucially on the nature of the scrambling of the one-electron states, and are model-dependent; the discussion of this issue is beyond the scope of the present paper. The experimental verification of Eq. (53), however, is possible without knowledge of $\langle [\delta \mathcal{U}_n^{(0)}(l)]^2 \rangle$. Since $\delta \mathcal{U}_n^{(0)}(l)$ is independent on the junction conductance, the difference between the values of $\langle [\delta \mathcal{U}_n(l)]^2 \rangle$ measured at various junction conductances can be directly compared to Eq. (53).

Equations (51) and (53) describe the behavior of $\langle \delta \mathcal{U}_n^2(l) \rangle$ in the limiting cases of small and large l respectively. The crossover between these two limits can be described analytically in the absence of scrambling of the electron wave functions by adding new electrons to the dot. Equations (13), (31) and (35) yield

$$\langle [\delta \mathcal{U}'_n(l)]^2 \rangle = \frac{32}{\beta} \left(\frac{\Delta}{E_C} \right)^2 \sum_{\alpha=L,R} \int_{\Delta}^{(1+l/2)\Delta} \frac{dD}{\Delta} \lambda_{\alpha}^2(D), \quad (54)$$

where $\lambda_{\alpha}(D)$ is given by Eq. (28). At small l , one can replace $\lambda_{\alpha}(D)$ in Eq. (54) with $\lambda_{\alpha}(\Delta) = \gamma'_{\alpha}$, which yields the l -dependent part of Eq. (51). For $l \sim E_C/\Delta$, one can replace $\lambda_{\alpha}(D)$ with $g_{\alpha}/(2\pi)^2$ within the most of the integration interval, so the right-hand-side of Eq. (54) matches Eq. (53).

IV. CROSSOVER BETWEEN WEAK AND STRONG TUNNELING

In the previous sections we considered the case of small enough conductances of both dot-lead contacts [the con-

dition (19) is satisfied]. In this weak tunneling regime, the n -th conductance peak corresponds to the resonant tunneling via the single, n -th level. The width of the peak is given by

$$\mathcal{W}_n \sim \frac{\max\{\Gamma_{nL} + \Gamma_{nR}, T\}}{E_C}, \quad (55)$$

where $\Gamma_{n\alpha}$ is the partial width of the n -th level with respect to the electron tunneling to the α -th lead. If the coupling of the dot to the leads is weak enough so the condition (18) is satisfied, the partial level widths are given by the conventional expression

$$\Gamma_{n\alpha} = g_\alpha \frac{|\psi_n(\mathbf{r}_\alpha)|^2}{\langle |\psi_n|^2 \rangle} \frac{\Delta}{2\pi}. \quad (56)$$

At larger values of $\sqrt{g_\alpha} \ln(E_C/\Delta)$, the level widths are renormalized (see Sec. II C):

$$\Gamma_{n\alpha} = [2\pi\mu_\alpha(\Delta)]^2 \frac{|\psi_n(\mathbf{r}_\alpha)|^2}{\langle |\psi_n|^2 \rangle} \frac{\Delta}{2\pi}. \quad (57)$$

It implies the renormalization of the junction conductance:

$$g_\alpha(D) = [2\pi\mu_\alpha(D)]^2, \quad (58)$$

where $\mu_\alpha(D)$ given by Eq. (28).

The position of a conductance peak is mainly determined by the position of the corresponding charge degeneracy point. However, there is another random contribution to the shift of the peak position, which stems from the randomness of the phases of the transmission amplitudes via different one-electron levels in the dot. Even when the dot is in the resonance, and the dominating contribution to the tunneling amplitude comes from a single resonant level, there is also a contribution from the cotunneling¹⁶ through the other levels, which yields the following estimate for the tunneling amplitude:

$$\begin{aligned} \mathcal{A}_n(\delta\mathcal{N}) &= e^{i\eta_n} \sqrt{\frac{\Gamma_{nL}\Gamma_{nR}}{[(\Gamma_{nL} + \Gamma_{nR})/2]^2 + (E_C\delta\mathcal{N})^2}} \\ &+ \sum_{k \neq n} e^{i\eta_k} \frac{\sqrt{\Gamma_{kL}\Gamma_{kR}}}{\varepsilon_k - \varepsilon_n + E_C\delta\mathcal{N}}, \end{aligned} \quad (59)$$

where η_k is the random phase of the amplitude of tunneling through the k -th level in the dot, and $\delta\mathcal{N}$ is the deviation from the closest charge degeneracy point. The position of the maximum of $|\mathcal{A}_n(\delta\mathcal{N})|$ given by Eq. (59), $\delta\mathcal{N} = \delta\mathcal{N}_n$, may not coincide with the point $\delta\mathcal{N} = 0$, *i.e.* the cotunneling contribution adds to the random shift of a peak. Equation (59), together with Eq. (57), yields the following estimate for the corresponding contribution to the peak spacing fluctuations:

$$\delta\mathcal{U}_n^{(\text{cotunn})} \sim \frac{\Delta}{E_C} [\mu_L^2(\Delta) + \mu_R^2(\Delta)]^3. \quad (60)$$

This contribution is much smaller than the one coming from the fluctuations of the charge degeneracy points [Eqs. (33), (33)], provided condition (19) is satisfied. This allowed us to neglect the contribution (60) yet so far.

Now we would like to extend our consideration beyond the limits set by Eq. (19). To demonstrate the new physical features emerging at stronger coupling of the dot to the leads, it is sufficient to limit ourselves to the case when the conductance of one channel (say, the right one) is small, and satisfies Eq. (18), as the other one (g_L) varies between 0 and 1. The consideration of the whole 2-dimensional parameter space $0 < g_L < 1$, $0 < g_R < 1$ would not add anything new to our understanding of the nature of the fluctuations of the conductance peak positions and will be omitted.

To begin with, we consider the conductance of the dot in the conditions opposite to the limit of weak coupling,

$$g_R \ll 1, \quad 1 - g_L \ll 1. \quad (61)$$

This case was studied in details in Ref. 17 and we first recall some findings of this work. Since one of the contacts is almost open, the charge of the dot is not quantized anymore. The Coulomb blockade is almost lifted and the notion of the charge degeneracy points is useless. Instead of sharp peaks, the conductance as a function of gate voltage \mathcal{N} exhibits oscillations with the period of unity. The oscillations occur around the value

$$\langle G \rangle = G_0 g_R \frac{\Delta}{E_C}, \quad (62)$$

the characteristic amplitude of the oscillations is also $G_0 g_R (\Delta/E_C)$. The phase of oscillations is a random quantity, varying with \mathcal{N} slowly (at scales larger than 1). The electron transport through the dot is mediated not by a single resonant level, as in the case of weak coupling, but by a set of levels, whose energies lie in the strip of the width E_C near the Fermi energy. As a result, the value of conductance at given gate voltage \mathcal{N} is determined by the properties of all levels in this set. Since there are no well-pronounced peaks, it is more natural to describe the statistical properties of conductance not in terms of the heights and positions of the conductance maxima, but rather in terms of the correlation functions $\langle G(\mathcal{N}_1)G(\mathcal{N}_2) \rangle$.

However, we still would like to study the statistical behavior of the conductance maxima, following the experiments,¹⁰ and in order to make a connection to the case of weak conductance. The quantitative consideration is hampered by the fact that, in the absence of sharp peaks, the exact positions of the conductance maxima are not associated with special points of any physical quantity. Therefore we will limit ourselves to a qualitative consideration of the fluctuations. It was mentioned above, that the Coulomb blockade is lifted when $g_L \approx 1$. Under these conditions, the conductance maxima occur at the points where the amplitudes of tunneling

via E_C/Δ levels in the dot add up most favorably [Cf. Eqs. (59), (60)]. The phase of transmission via each level, η_k , depends on the gate voltage, so the function $G(\mathcal{N})$ is not constant. It is (almost) periodic, because the functions $\eta_k(\mathcal{N})$ have period of unity; $G(\mathcal{N})$ is not exactly periodic because when the gate voltage \mathcal{N} is shifted by unity, one level is replaced in the set which mediates conductance. Therefore, the conductance maxima are not equally spaced, but their positions fluctuate with respect to each other. When \mathcal{N} is varied by E_C/Δ , all the “conducting” levels are replaced, so $G(\mathcal{N})$ is not correlated with $G(\mathcal{N} + E_C/\Delta)$. In particular, the positions of the maxima separated by E_C/Δ other maxima fluctuate independently within range $\delta\mathcal{N}_n \sim 1$ each. Therefore, the characteristic amplitude of fluctuations of the spacing between nearest maxima equals

$$\delta\mathcal{U}_n \sim \sqrt{\frac{\Delta}{E_C}} \quad (63)$$

for the conditions defined in Eq. (61).

Now we can combine the knowledge acquired in the consideration of the case of weak [Eq. (19)] and strong [Eq. (61)] tunneling through the left contact, to deal with the case of the intermediate conductance

$$\left[\frac{\pi}{\ln(E_C/\Delta)} \right]^2 < g_L < 1. \quad (64)$$

In considerations of Sec. II we used the renormalization group transformation of the Hamiltonian only in the very vicinity of the conductance peak. In principle, this transformation can be performed at any value of $\delta\mathcal{N}$, where $\delta\mathcal{N}$ is the distance to the closest charge degeneracy point of Hamiltonian (1). If

$$|\delta\mathcal{N}| > \exp(-\pi/\sqrt{g_L}), \quad (65)$$

then the renormalization must be stopped when the reduced band width D reaches $E_C|\delta\mathcal{N}|$. Indeed, if $D < E_C|\delta\mathcal{N}|$, then one of the two dot’s charge states is left beyond the band limits; only one charge state is then possible. One can see that the renormalization defined by Eq. (21) does not bring the system out of the conditions of weak coupling, because $g_L(D = E_C|\delta\mathcal{N}|)$ is still much less than unity. The conductance of the dot can then be estimated from $\hat{H}(D = E_C|\delta\mathcal{N}|)$ with the help of the formula for elastic cotunneling. Under the condition (65), the conductance is

$$G \sim G_0 g_R g_L(D) \frac{\Delta}{D}, \quad \text{with } D = E_C|\delta\mathcal{N}|. \quad (66)$$

The renormalization of the conductance of the right contact, g_R , can be neglected, since it satisfies Eq. (18).

If, on the contrary,

$$|\delta\mathcal{N}| < \exp(-\pi/\sqrt{g_L}), \quad (67)$$

then the renormalization is stopped when D reaches $E_C \exp(-\pi/\sqrt{g_L})$. At this point, the renormalized conductance of the left contact, given by Eq. (58), becomes of the order of unity. Then the scaling law (21), based on the perturbation theory in the small parameter $g_L(D)$, is not applicable. The nature of conductance through the dot with such parameters (one contact is almost open, the other one is almost closed) was discussed earlier in this section. The characteristic conductance for the conditions of Eq. (65) is given by the formula similar to Eq. (62). In this formula, E_C , which in Eq. (62) plays the role of the width of the band of electrons affected by the charging, must be replaced with $D = E_C \exp(-\pi/\sqrt{g_L})$:

$$G \sim G_0 g_R \frac{\Delta}{E_C} \exp\left(\frac{\pi}{\sqrt{g_L}}\right). \quad (68)$$

This value is parametrically larger than the one given by Eq. (66). Thus the characteristic width of a conductance peak in the conditions of Eq. (64) is

$$\mathcal{W}_n \sim \exp\left(-\frac{\pi}{\sqrt{g_L}}\right). \quad (69)$$

The conductance maxima are not tied to the charge degeneracy points. Instead, their positions determined by the interference of the amplitudes of transmission through $(E_C/\Delta) \exp(-\pi/\sqrt{g_L})$ levels, that belong to the reduced band of width $E_C \exp(-\pi/\sqrt{g_L})$. Therefore, the conductance may have a maximum, roughly speaking, at any point lying in the interval where the renormalized conductance of the left contact is close to unity, *i.e.*, within the region defined by $|\delta\mathcal{N}| < \exp(-\pi/\sqrt{g_L})$. The positions of the maxima corresponding to two neighboring charge degeneracy points are correlated, because they are defined by the same set of levels except for one. This situation is similar to that in the case when one of the contacts *initially* had conductance close to unity. The difference is that now the set of the levels which determines the position of a maximum is smaller. Employing the same ideas we used for the dot with one contact initially almost open, we obtain that the characteristic amplitude of fluctuations of the maxima spacings is

$$\delta\mathcal{U}_n \sim \sqrt{\frac{\Delta}{E_C}} \exp\left(-\frac{\pi}{2\sqrt{g_L}}\right), \quad (70)$$

for the conditions defined by Eq. (64). This expression matches Eqs. (44) and (63) at $g_L \sim [\pi/\ln(E_C/\Delta)]^2$ and $g_L \sim 1$, respectively.

Equation (70) gives an estimate for the fluctuations of spacing between two neighboring maxima. Now we extend this estimate to distant maxima. As we discussed before in this Section, the random positions of the conductance maxima are determined by the sets of $\sim (E_C/\Delta) \exp(-\pi/\sqrt{g_L})$ levels. For the n -th and $(n+l)$ -th maxima, the levels in these two sets are the same except for l of them. These l levels in each of the two sets produce uncorrelated contributions to the positions

of the two maxima. This contribution grows with l , since the contribution of each particular level is independent of the others:

$$\delta\mathcal{U}_n(l) \sim \sqrt{l} \sqrt{\frac{\Delta}{E_C}} \exp\left(-\frac{\pi}{2\sqrt{g_L}}\right), \quad (71)$$

$$\text{for } l < \frac{E_C}{\Delta} \exp\left(-\frac{\pi}{\sqrt{g_L}}\right).$$

At $l > (E_C/\Delta) \exp(-\pi/\sqrt{g_L})$ there are no common levels in the two sets, and the fluctuations of the positions of the n -th and $(n+l)$ -th peaks are independent. The variance of spacing between them saturates at large l :

$$\delta\mathcal{U}_n(l) \sim \exp\left(-\frac{\pi}{\sqrt{g_L}}\right), \quad (72)$$

$$\text{for } l > \frac{E_C}{\Delta} \exp\left(-\frac{\pi}{\sqrt{g_L}}\right).$$

The levels that are eliminated by the reduction of the band down to $E_C \exp(-\pi/\sqrt{g_L})$ in the course of renormalization also make a contribution to $\delta\mathcal{U}_n(l)$. However, it is important only in the narrow region of crossover between the regimes of weak [Eqs. (54), (53)] and intermediate [Eqs. (71), (72)] conductance, where the number of levels in the reduced band is of the order of unity. Otherwise this contribution is small, as compared to the one given by Eq. (71), and can be neglected.

V. CONCLUSION

We have studied the statistical properties of the spacings between the conductance peaks in a partially open

Coulomb blockaded quantum dot. We found that the fluctuations of the electron wave functions in the dot contribute to the fluctuations of the peak spacings; this contribution grows with the conductance of the contacts, see Table I.

For relatively weak coupling of the dot to the leads, $g_{L,R} < [\pi/\ln(E_C/\Delta)]^2$, the peak conductance is mediated by a single electron level, and the peaks are sharp. The variance of the peak spacing fluctuations for the neighboring peaks is given by Eqs. (44); it reaches Δ^2 when $g_{L,R} \sim [\pi/\ln(E_C/\Delta)]^2$.

At larger values of $g_{L,R}$, the conductance peaks are broad, and many levels are involved in the transport through the dot. Thus the properties of conductance peaks (more precisely, maxima) are determined by the wave functions of many electron states. The variance of the spacing between the maxima continues to grow with the conductance of contacts, and is given by Eq. (70).

The fluctuations of the spacing between two conductance peaks grow with the distance between them, see Eqs. (51), (71). At large distances between two peaks, the variance of the spacing between them saturates at the value given by Eq. (53) (72).

The dependence of the peak position on the one-electron wave functions in the dot leads to the correlations between the fluctuations in the peaks' spacings and heights: the spacings between the higher peaks are, on average, smaller. The parameter characterizing this correlation is given by Eq. (48).

TABLE I. The characteristic values of the peak width and the amplitude of fluctuations of the spacing between the neighboring peaks in units of E_C for $g_R \ll 1$, $g_R < g_L < 1$, as given by Eqs. (44), (57), (69), (70). The numeric factors are omitted.

conductance of the contacts	peak width	$\sqrt{\langle \delta\mathcal{U}_n^2 \rangle}$
$g_R < g_L < \left[\frac{\pi}{\ln(E_C/\Delta)}\right]^2$	$\frac{\Delta}{E_C} g_L$	$\frac{\Delta}{E_C} \sqrt{g_L} \tan\left(\frac{1}{\pi} \sqrt{g_L} \ln \frac{E_C}{\Delta}\right)$
$\left[\frac{\pi}{\ln(E_C/\Delta)}\right]^2 < g_L < 1, \quad g_R < g_L$	$\exp\left(-\frac{\pi}{\sqrt{g_L}}\right)$	$\sqrt{\frac{\Delta}{E_C}} \exp\left(-\frac{\pi}{2\sqrt{g_L}}\right)$

ACKNOWLEDGMENTS

This work has been supported by the NSF Grant No. DMR-9731756. The discussions with C.M. Marcus are gratefully acknowledged.

¹ M.A. Kastner, Rev. Mod. Phys. **64**, 849 (1992).

² M.L. Mehta, *Random Matrices*, 2nd ed. (Academic Press, London, 1991).

³ R.A. Jalabert, A.D. Stone, and Y. Alhassid, Phys. Rev. Lett. **68**, 3468 (1992).

⁴ A.M. Chang *et al.*, Phys. Rev. Lett. **76**, 1695 (1996); J.A. Folk *et al.*, *ibid.* **76**, 1699 (1996); S.M. Cronenwett *et al.*, *ibid.* **79**, 2312 (1997).

⁵ U. Sivan *et al.*, Phys. Rev. Lett. **77**, 1123 (1996).

⁶ F. Simmel, T. Heinzel, and D.A. Wharam, Europhys. Lett.

- 38**, 123 (1997); F. Simmel *et al.*, Phys. Rev. B **59**, R10441 (1999).
- ⁷ S.R. Patel *et al.*, Phys. Rev. Lett. **80**, 4522 (1998).
- ⁸ See P.N. Walker, Y. Gefen, G. Montambaux, Phys. Rev. Lett. **82**, 5329 (1999) and references therein.
- ⁹ R.O. Vallejos, C.H. Lewenkopf, E.R. Mucciolo, Phys. Rev. Lett. **81**, 677 (1998).
- ¹⁰ S.M. Maurer *et al.*, Phys. Rev. Lett. **83**, 1403 (1999).
- ¹¹ P.W. Anderson, J. Phys. C **11**, 5015 (1978).
- ¹² L.I. Glazman and K.A. Matveev, Sov. Phys. JETP **71**, 1031 (1990); K.A. Matveev *ibid.* **72**, 892 (1991).
- ¹³ C.W.J. Beenakker, Phys. Rev. B **44**, 1646 (1991).
- ¹⁴ These quantities are analogous to the corrections to the energy levels of an Anderson impurity, and were calculated in: F.D.M. Haldane, Phys. Rev. Lett. **40**, 416 (1978).
- ¹⁵ S.R. Patel *et al.*, Phys. Rev. Lett. **81**, 5900 (1998); D.R. Stewart *et al.*, Science **278**, 1784 (1997).
- ¹⁶ D.V. Averin, Yu.V. Nazarov, Phys. Rev. Lett. **65**, 2446 (1990).
- ¹⁷ I.L. Aleiner, L.I. Glazman, Phys. Rev. B **57**, 9608 (1998).